The Astrophysical Journal Supplement Series, 258:35 (5pp), 2022 February https://doi.org/10.3847/1538-4365/ac4988

Experimental and Theoretical Radiative Parameters of Highly Excited Levels in Re II

Meina Liu[1], Huiting Ma[1], Yidan Geng[1], Patrick Palmeri[2], Pascal Quinet[2,3], and Zhenwen Dai[1]
[1] College of Physics, Jilin University, Changchun 130012, People's Republic of China; dai@jlu.edu.cn
[2] Physique Atomique et Astrophysique, Université de Mons, B-7000 Mons, Belgium; pascal.quinet@umons.ac.be
[3] IPNAS, Université de Liège, B-4000 Liège, Belgium
Received 2021 September 25; revised 2021 November 12; accepted 2021 December 15; published 2022 February 1

Abstract

Natural radiative lifetimes of 22 odd-parity levels of Re II in the energy range between 43,937.7 and 65,572.3 cm^{-1} were measured by the time-resolved laser-induced fluorescence method. To our knowledge, the lifetimes for 18 out of 22 levels were measured for the first time. The theoretical radiative lifetimes and branching fractions (BFs) for these levels were obtained from pseudorelativistic Hartree–Fock calculations including core-polarization effects. By combining the experimental lifetimes and calculated BFs, a set of semiempirical transition probabilities and oscillator strengths for 232 Re II lines were determined. The radiative parameters obtained in the present work will greatly enrich the atomic database of Re II and hence are expected to be helpful for astrophysicists in Re abundance evaluation of stars.

Unified Astronomy Thesaurus concepts: Radiative processes (2055); Transition probabilities (2074); Atomic physics (2063); Atomic spectroscopy (2099)

Supporting material: machine-readable table

1. Introduction

Accurate abundance determinations of heavy neutron-capture elements are required in astrophysics for understanding the role of the *s* (slow) and *r* (rapid) processes in the buildup of heavy nuclei nucleosynthesis (Palmeri et al. 2006). This process is made possible only if reliable radiative data, such as lifetimes, branching fractions (BFs), transition probabilities, and oscillator strengths, are available for the transitions of astrophysical interest. Singly ionized rhenium (Re II) lines have been observed in many stars, e.g., the chemically peculiar (CP) star HD 65949 (Cowley et al. 2010), the uranium-rich metal-poor star CS 31082-001 (Siqueira Mello et al. 2013), the A1 Vm star Sirius (Cowley et al. 2016), and the hot Am star HR 3383 (Wahlgren et al. 2021) etc. Due to a large nuclear magnetic moment in Re, the Re II lines in stellar spectra are usually broadened by hyperfine structure (HFS) and hence their oscillator strengths are parceled among various HFS components. In this case, if HFS is neglected the Re abundance will be overestimated (Wahlgren et al. 1997). However, there is a serious lack of data on the radiative parameter and HFS for Re II. Therefore, the present work intends to extend radiative data for Re II.

Terrestrial rhenium consists of two stable isotopes, ^{185}Re and ^{187}Re, with relative abundances of 37.4% and 62.6% and a common nuclear spin 5/2 (Haynes 2016). To the best of our knowledge, transition probabilities and oscillator strengths of Re II were first reported by Corliss & Bozman (1962), but it is now well established that these data contain large systematic errors (Palmeri et al. 2005). Later, radiative data of Re II were measured by Wahlgren et al. (1997) who reported an absolute transition probability for Re II 2275.253 Å, obtained from the lifetime of the $z^7P^\circ_2$ level by the time-resolved laser-induced fluorescence (TR-LIF) method and an experimental BF determined by observing emission from a hollow cathode discharge lamp with a grating monochromator equipped with a photomultiplier tube (PMT). Henderson et al. (1999) used the beam-foil method to measure the lifetimes of $z^7P^\circ_{2,3}$ in Re II, and determined the oscillator strengths of two transitions by combining with the BFs deduced from the emission measurements by Corliss & Bozman (1962). Palmeri et al. (2005) reported the experimental and calculated lifetime values of seven odd-parity levels in the range of 43,937.578–57,138.6 cm^{-1} by the TR-LIF technique and the pseudorelativistic Hartree–Fock method including core-polarization effects (HFR+CPOL), respectively, and transition probabilities for 45 transitions of Re II using a combination of experimental radiative lifetime values and theoretical BFs, as part of the general project to build the database Database for the Sixth Row Elements (Fivet et al. 2007). Using the HFR+CPOL method, Cowley et al. (2010) presented calculated values of oscillator strengths for 176 Re II lines. Ortiz et al. (2013) measured experimental transition probabilities for 37 spectral lines of Re II by laser-induced breakdown spectroscopy, 15 of which were reported for the first time.

As far as we know, the lifetimes of a total of only seven levels in Re II in the range of 43,937.7–57,138.6 cm^{-1} have been measured before. Excluding the experimental values of Corliss & Bozman (1962), experimental transition probabilities or oscillator strengths of 37 lines, semiempirical values of 45 lines, and theoretical values of 176 lines have been reported. In the present work, we measured the radiative lifetimes of 22 highly excited levels of Re II lying in the energy range 43,937.7–65,572.3 cm^{-1} by the TR-LIF method and 18 of them are reported for the first time. In addition, the lifetime data reported in this work were combined with BFs obtained from HFR+CPOL calculations to derive transition probabilities (*gA*) and oscillator strengths (log(*gf*)) for 232 Re II lines. Some of these spectral lines have been observed in stellar spectra. For example, the lines 3303.21, 3365.43, 3379.07, 3403.73, 3580.14, 3647.57, and 3742.30 Å were identified in the spectra

Table 1
Measured and Calculated Lifetimes of Re II Highly Excited Levels and Comparison with Previous Results

Upper Level[a]		Lower Level[a]		$\lambda_{Exc.}$	$\lambda_{Obs.}$	Lifetime (ns)			
						This Work		Previous	
Assignment	E (cm^{-1})	J	E (cm^{-1})	(nm)	(nm)	Exp.	Calc.	Exp.	Calc.
$5d^5(^6S)6p\ z^7P^\circ_2$	43,937.7	3	0.0	227.595	228	4.3(3)		4.47(22)[b], 5.1(8)[c], 4.5(3)[d,e]	3.98[d], 4.0[e]
$5d^5(^6S)6p\ z^7P^\circ_3$	45,147.5	2	14,352.2	324.725	693	4.6(2)		6.7(8)[c], 4.6(3)[d,e]	4.03[d], 4.0[e]
$5d^5(^4F)6p\ z^5D^\circ_1$	56,372.1	0	13,777.3	234.770	255	8.5(3)	9.4		
$5d^5(^4F)6p\ z^5F^\circ_3$	57,050.2	2	14,352.2	234.203	251	7.2(4)		6.5(4)[d,e]	3.73[d], 3.7[e]
$5d^5(^4F)6p\ z^5D^\circ_2$	57,138.6	2	14,352.2	233.719	261	8.2(8)		8.3(5)[d,e]	4.88[d], 4.9[e]
$5d^5(^4F)6p\ z^5D^\circ_3$	59,329.9	4	14,882.6	224.986	237	4.6(6)	3.4		
$5d^5(^4P)6p\ z^3P^\circ_2$	59,388.3	1	14,824.0	224.395	234	6.5(4)	3.8		
$5d^5(^4F)6p\ z^5F^\circ_4$	59,596.1	4	14,882.6	223.646	234	7.2(6)	6.4		
596°_3	59,665.8	4	14,882.6	223.298	236	6.1(3)	5.4		
604°_1	60,487.2	0	13,777.3	214.087	264	9.2(2)	19.0[f]		
620°_2	62,057.3	3	14,930.5	212.193	272	12.1(5)	14.4		
627°_1	62,717.8	1	14,824.0	208.795	220	6.3(3)	5.1		
$5d^5(^4F)6p\ z^5D^\circ_4$	62,859.0	4	14,882.6	208.436	208	4.4(4)	3.2		
629°_3	62,914.9	3	14,930.5	208.401	219	9.5(4)	9.0		
630°_3	63,043.3	3	14,930.5	207.845	218	5.9(3)	4.2		
631°_4	63,127.7	4	14,882.6	207.275	207	10.9(4)	9.2		
634°_2	63,464.2	3	14,930.5	206.042	248	6.3(3)	4.5		
$5d^5(^4F)6p\ z^5F^\circ_5$	64,282.3	4	14,882.6	202.430	202	4.1(4)	3.3		
644°_2	64,411.4	2	17,223.5	211.919	234	7.9(3)	4.8		
6494°_3	64,942.2	2	17,223.5	209.561	225	7.1(4)	4.4		
650°_1	65,011.0	2	17,223.5	209.260	239	4.6(4)	3.7		
655°_3	65,572.3	2	17,223.5	206.830	258	5.2(4)	3.6		

Notes.
[a] Moore (1971). The assignments of some levels with just numbers are from the NIST database (Kramida et al. 2020).
[b] Wahlgren et al. (1997).
[c] Henderson et al. (1999).
[d] Palmeri et al. (2005).
[e] Fivet et al. (2007).
[f] Main decay channels are affected by strong cancellation effects (CF < 0.05).

of the CP star HD 65949[4] (Cowley et al. 2008). Our new data can be used to derive Re abundances through these lines.

2. Lifetime Measurements

The experimental setup used for the lifetime measurement has been presented by Tian et al. (2016), so only a brief description is given here. One 532 nm Q-switched Nd:YAG laser with a 10 Hz repetition rate and about an 8 ns pulse duration was focused vertically onto the surface of a rotating rhenium target placed inside a vacuum chamber to produce laser plasma. The other 532 nm Q-switched Nd:YAG laser (Spectra-Physics Quanta-Ray) working at a 10 Hz repetition rate with about an 8 ns duration was employed to pump a dye laser (Sirah Cobra-Stretch) with DCM or Rhodamine 640 dyes. To obtain the required excitation laser wavelength, the second or the third harmonic of the dye laser was produced by one or two β-barium borate type-I crystals, and sometimes the third harmonic of the dye laser was focused into a stimulated Raman-scattering cell with H_2 to obtain the first-order Stokes component of Raman shifting. Then the excitation laser was horizontally sent into the vacuum chamber where it intersected the Re plasma about 8 mm above the target surface. The delay between the excitation and ablation pulses was adjusted by a digital delay generator (SRS DG535).

In the measurements, we must make sure that only the studied level was correctly excited. For this purpose, we monitored the dye laser wavelength by a high-precision wavemeter (HighFinesse WS6). Besides that, some systematic effects such as the radiation trapping, the flight-out-of-view, saturation, and collision effects, which can induce additional errors on lifetime measurement, were carefully minimized (Wang et al. 2018). To wash out quantum beats caused by the Earth's magnetic field, a 100 G magnetic field produced by a pair of Helmholtz coils in a horizontal direction was applied.

3. Theoretical Branching Fractions and Semiempirical Transition Probabilities

The present theoretical BFs and lifetimes have been determined from theoretical transition probabilities obtained using the atomic structure model of Palmeri et al. (2005). In the latter, the pseudorelativistic Hartree–Fock (HFR) method of Cowan (1981) corrected to include the core-polarization interactions through a polarization potential and a correction to the dipole operator (CPOL) (Quinet et al. 1999) was employed semi-empirically to compute the atomic level energies and wave functions. The details about the HFR +CPOL model can be found in Palmeri et al. (2005) and will therefore only be summarized here.

In these calculations, the core–valence correlations have been modeled using a core-polarization potential and a correction to the electric dipole transition operator, following

[4] http://websites.umich.edu/~cowley/hd65949/re_new.html

Table 2
Branching Fractions, Transition Probabilities, Oscillator Strengths Obtained in the Present Work for Highly Excited Levels of Re II, and Comparison with Previous Results

Upper Level[a]		Lower Level[a]		λ[b]	BF[c]	gA (10^6 s^{-1})			Log(gf)		
Assign.	E (cm^{-1}) Lifetime (ns)	Assign.	E (cm^{-1})	(nm)		This Work[d]	Previous		This Work[d]	Previous	
							Exp.[e]	Calc.[f]		Exp.[g]	Calc.[h]
$5d^5(^6S)6p\ z^7P^o_2$	43937.7	$5d^5(^6S)6s\ a^7S_3$	0.0	227.525	0.931 (B)	1080 (B)	1030(170)	1030	−0.07 (B)	−0.28(3)	−0.04
	$\tau = 4.3(3)$	$5d^46s^2\ a^5D_2$	14,352.2	337.908	0.038 (E)	43.8 (E)	53.9(84)	40	−1.12 (E)		−1.09
		$5d^5(^6S)6s\ a^5S_2$	17,223.5	374.228	0.011 (E)	12.6 (E)	16.6(29)	10	−1.57 (E)		
$5d^5(^6S)6p\ z^7P^o_3$	45147.5	$5d^5(^6S)6s\ a^7S_3$	0.0	221.428	0.852 (B)	1300 (B)	1230(200)	1300	−0.02 (B)	−1.05(10)	0.04
	$\tau = 4.6(2)$	$5d^46s^2\ a^5D_2$	14,352.2	324.632	0.011 (E)	17.3 (E)	27.8(54)	20	−1.56 (E)		
		$5d^46s^2\ a^5D_4$	14,882.6	330.321	0.039 (E)	59.0 (E)		60	−1.01 (E)		−0.95
		$5d^46s^2\ a^5D_3$	14,930.5	330.845	0.018 (E)	27.2 (E)	58.5(90)	30	−1.35 (E)		
		$5d^5(^6S)6s\ a^5S_2$	17,223.5	358.013	0.067 (E)	102 (E)	110(20)	100	−0.70 (E)		−0.64

Notes.
[a] Moore (1971). The assignments of some levels with just numbers are from the NIST database (Kramida et al. 2020).
[b] Wavelengths above 200 nm are listed as air wavelengths and below as vacuum wavelengths. The vacuum wavelengths are Ritz wavelengths deduced from experimental energy level values from the compilation by Moore (1971), while the air wavelengths are converted from the vacuum ones.
[c] BFs calculated using the HFR+CPOL method. Only BF values greater or equal to 0.01 are given. The estimated uncertainties are given between parentheses using the same code letter as the one used in the NIST database (Kramida et al. 2020), i.e., B (⩽10%), C+ (⩽18%), C (⩽25%), D+ (⩽40%), D (⩽50%) and E (>50%) (see text).
[d] gA and log gf values obtained in this work were deduced from the combination of HFR+CPOL branching fractions with experimental lifetimes. The estimated uncertainties are given between parentheses. They are indicated by the same code letter as the one used in the NIST database (Kramida et al. 2020), i.e., B (⩽10%), C+ (⩽18%), C (⩽25%), D+ (⩽40%), D (⩽50%) and E (>50%) (see text).
[e] Ortiz et al. (2013).
[f] Palmeri et al. (2005). Determined by combining the measured lifetimes with the calculated BF.
[g] Henderson et al. (1999).
[h] Cowley et al. (2010).
[i] Sansonetti & Martin (2005).

(This table is available in its entirety in machine-readable form.)

the methodology described in detail by Quinet et al. (1999, 2002). A $4f^{14}$ Er-like Re VIII ionic core surrounded by six valence electrons has been chosen. The core-polarization parameters, namely the dipole polarizability, α_d, and the cutoff radius, r_c, were chosen to be equal to 2.58 a_0^3 and 1.22 a_0, respectively. The former value is the result of the extrapolation along the erbium isoelectronic sequence of α_d parameters tabulated by Fraga et al. (1976) for Tm II, Yb III, Lu IV, and Hf V while the latter value corresponds to the HFR mean radius of the outermost core orbital (5p). As regards the valence–valence correlations, we explicitly considered the interactions between the following configurations: $5d^5ns$, $5d^46sns$, $5d^6$, $5d^56d$, $5d^46s6d$, $5d^36s^26d$, $5d^46p^2$, and $5d^36s6p^2$ with $n = 6$–8 for the even parity; $5d^5np$, $5d^46snp$, and $5d^36s^26p$ with $n = 6$–8 for the odd parity. In addition, some radial parameters representing the electrostatic and spin–orbit interactions within and between the configurations $5d^56s$, $5d^46s^2$, $5d^6$, $5d^56p$, and $5d^46s6p$ have been adjusted so as to improve the agreement between the computed eigenvalues and the available experimental energy levels (Meggers et al. 1958; Wyart 1977; Wahlgren et al. 1997) using a well-established least-squares fitting process implemented in the Cowan (1981) suite of computer codes. This allowed us to reproduce the experimental energy level values with standard deviations of 135 and 192 cm^{-1} in the even and odd parities, respectively. In Palmeri et al. (2005)'s paper, this HFR+CPOL model has been found to give a very good agreement (within a few percent) when comparing the calculated radiative lifetimes with those experimentally measured using the laser-induced fluorescence technique. It is also worth mentioning that the HFR+CPOL method has proven its ability to reproduce accurate lifetime measurements obtained by laser spectroscopy in a very large amount of different neutral and lowly ionized heavy atoms, as described in the review article by Quinet (2017), for example.

Consequently, the same physical model has been used in the present work in order to extend the set of atomic decay parameters for the transitions from the present measured energy levels reported in Table 1. In this table, our theoretical lifetime of the level 604°_1 is affected by strong cancellation effects, i.e., with cancellation factors (CFs) as defined in Cowan (1981), less than 5%, on the line strength of the main decay channels and therefore appears with a value far lower than the experimental one. Concerning the other levels, the agreements between our TR-LIF lifetimes and their corresponding HFR+CPOL values are on average of the order of 30%, the calculated values being almost systematically slightly smaller than the experimental ones. This systematic deviation is probably due to a slight underestimation of the effects of the core–valence electronic interaction, which was evaluated by a core-polarization potential up to $5p^6$ while the 5d orbital was still occupied by a few electrons in the list of configurations explicitly introduced in the calculations. Our HFR+CPOL BFs are presented in Table 2 for the main decay channels having BF values greater or equal to 0.01. In this table, the corresponding transition probabilities and oscillator strengths have been derived by combining our HFR+CPOL BFs with our TR-LIF lifetimes. The estimated uncertainties as reported in Table 2 are assumed to be 20%, 30%, 35%, 40%, and 55% for BF = 0.8–1.0, 0.6–0.8, 0.4–0.6, 0.2–0.4, and 0.1–0.2, respectively (Wang et al. 2019). These uncertainties were then combined in quadrature with the experimental lifetime uncertainties derived from our measurements to yield the uncertainties of *gA* and *gf* values.

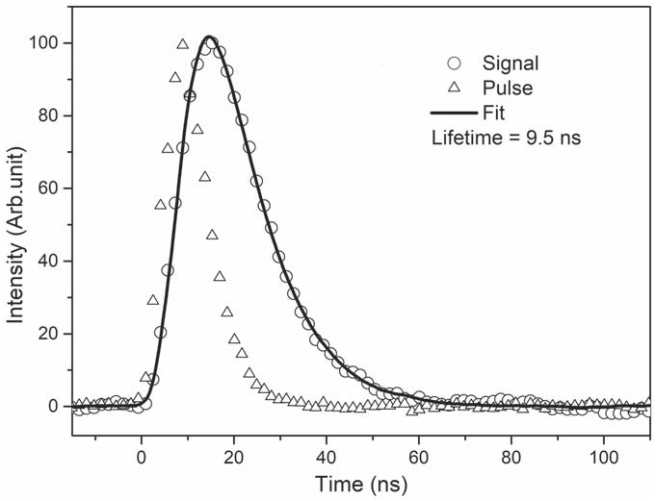

Figure 1. A typical fluorescence decay curve of the Re II level 62,914.9 cm^{-1} with the fitted convolution curve between the laser pulse and an exponential.

4. Results and Discussion

The lifetime values were extracted by a convolutional fit of a fluorescence decay curve and an exciting pulse. For example, a fluorescence decay curve with a convolution fit is shown in Figure 1. The radiative lifetimes of 22 levels from 43,937.7 to 65,572.3 cm^{-1} in Re II measured in this work are presented in Table 1. Their uncertainties consist of the systematic errors and the statistical errors from different recordings (Shang et al. 2015). The measured results are in the range of 4.1–12.1 ns with uncertainties less than 10% except for the level 59,329.9 cm^{-1} that has an uncertainty of 13.1%. To the best of our knowledge, the lifetimes for 18 levels were measured for the first time. For the four levels previously reported, our results are in good agreement with the results presented by Wahlgren et al. (1997), Palmeri et al. (2005), and Fivet et al. (2007) using the TR-LIF method, respectively. The lifetime values of the 43,937.7 and 45,147.5 cm^{-1} levels reported by Henderson et al. (1999) using the beam-foil method, which may involve cascade population to studied levels and hence prolong their decay time if cascade correction is not well done, are systematically larger than our results and the results in the literature (Wahlgren et al. 1997; Palmeri et al. 2005; Fivet et al. 2007). The differences (Ours − Henderson)/Ours are 18.6% and 45.7% for the two levels, respectively.

BFs, semiempirical transition probabilities, and oscillator strengths obtained in this work for highly excited levels of Re II are listed in Table 2. They correspond to 232 Re II spectral lines appearing in the wavelength range of 153–375 nm. The previously reported results are also presented for comparison. The good agreement (within 20%) between our present *gA* and log(*gf*) values and those of both Palmeri et al. (2005) and Cowley et al. (2010) are not surprising as all three based are on the same HFR+CPOL model. They only differ in the normalization with different lifetime measurements or, in Cowley et al. (2010), the transition probabilities and oscillator strengths were not renormalized and are therefore "pure" HFR+CPOL values. Concerning the comparison with the two experimental oscillator strengths of Henderson et al. (1999), these were determined using BF values derived from the transition probabilities measured by Corliss & Bozman (1962), but it is well established that these old arc measurements contain large systematic errors. Indeed, there is a 1 dex

difference between our log(gf) value for the strong line $5d^5(^6S)6s\ a^7S_3$–$5d^5(^6S)6p\ z^7P^\circ_3$ and the value determined by Henderson et al. (1999). In that respect, the good agreements within the uncertainties reported in Table 2 between the transition probabilities as estimated in this work and from the measurements of Ortiz et al. (2013) are reassuring, notably for this abovementioned transition.

5. Conclusions

In conclusion, the radiative lifetimes of 22 excited states in Re II were measured with the TR-LIF method and the BFs for 232 transitions were determined by HFR+CPOL calculations. By combining the experimental lifetimes and calculated BFs, the transition probabilities and oscillator strengths for 232 transitions in Re II were presented. These atomic radiative data are useful for astrophysical spectra analyses and for insights into transition dynamics of this ion.

This work was supported by the National Natural Science Foundation of China (grant No. U1832114). P.P. and P.Q. are, respectively, the Research Associate and Research Director of the Belgian National Fund for Scientific Research (F.R.S.-FNRS) whose financial support is greatly appreciated.

ORCID iDs

Zhenwen Dai https://orcid.org/0000-0002-9040-2315

References

Corliss, C. H., & Bozman, W. R. 1962, Experimental Transition Probabilities for Spectral Lines of Seventy Elements (Washington, DC: U.S. GPO)
Cowan, R. D. 1981, The Theory of Atomic Structure and Spectra (Berkeley, CA: Univ. California Press)
Cowley, C. R., Ayres, T. R., Castelli, F., et al. 2016, ApJ, 826, 158
Cowley, C. R., Hubrig, S., Palmeri, P., et al. 2010, MNRAS, 405, 1271
Cowley, C. R., Hubrig, S., & Wahlgren, G. M. 2008, JPhCS, 130, 012005
Fivet, V., Quinet, P., Palmeri, P., Biémont, É., & Xu, H. L. 2007, JESRP, 156, 250
Fraga, S., Karwowski, J., & Saxena, K. M. S. 1976, Handbook of Atomic Data (Amsterdam: Elsevier)
Haynes, W. M. 2016, CRC Handbook of Chemistry and Physics (97th ed.; Boca Raton, FL: CRC Press)
Henderson, M., Irving, R. E., Matulioniene, R., et al. 1999, ApJ, 520, 805
Kramida, A., Ralchenko, Y., Reader, J. & NIST ASD Team 2020, NIST Atomic Spectra Database v5.8 (Gaithersburg, MD: National Institute of Standards and Technology)
Meggers, W. F., Catalan, M. A., & Sales, M. 1958, JRNBS, 61, 441
Moore, C. E. 1971, Atomic Energy Levels as Derived from the Analysis of Optical Spectra—Molybdenum through Lanthanum and Hafnium through Actinium, Vol. 3 (Gaithersburg, MD: National Bureau of Standards)
Ortiz, M., Aragón, C., Aguilera, J. A., Rodríguez-García, J., & Mayo-García, R. 2013, JPhB, 46, 185702
Palmeri, P., Quinet, P., Biémont, É., Svanberg, S., & Xu, H. L. 2006, PhyS, 74, 297
Palmeri, P., Quinet, P., Biémont, É., Xu, H. L., & Svanberg, S. 2005, MNRAS, 362, 1348
Quinet, P. 2017, CaJPh, 95, 790
Quinet, P., Palmeri, P., Biémont, E., et al. 1999, MNRAS, 307, 934
Quinet, P., Palmeri, P., Biémont, E., et al. 2002, JAllC, 344, 255
Sansonetti, J. E., & Martin, W. C. 2005, JPCRD, 34, 1559
Shang, X., Wang, Q., Zhang, F. F., Wang, C., & Dai, Z. W. 2015, JQSRT, 163, 34
Siqueira Mello, C., Spite, M., Barbuy, B., et al. 2013, A&A, 550, A122
Tian, Y. S., Wang, X. H., Yu, Q., et al. 2016, MNRAS, 457, 1393
Wahlgren, G. M., Johansson, S. G., Litzén, U., et al. 1997, ApJ, 475, 380
Wahlgren, G. M., Nielsen, K. E., & Leckrone, D. S. 2021, MNRAS, 500, 2451
Wang, Q., Gamrath, S., Palmeri, P., et al. 2019, JQSRT, 225, 35
Wang, X. H., Quinet, P., Li, Q., et al. 2018, JQSRT, 212, 112
Wyart, J.-F. 1977, Opt. Pura Apl., 10, 177